# Multinuclear Cobalt(II)-Containing Heteropolytungstates: Structure, Magnetism, and Electrochemistry

Masooma Ibrahim,[†,§,¶] Ali Haider,[†,§] Yanhua Lan,[‖] Bassem S. Bassil,[†] Akina M. Carey,[†] Rongji Liu,[⊥,#] Guangjin Zhang,[⊥] Bineta Keita,[▽] Wenhui Li,[⊥,◆] George E. Kostakis,[⊗] Annie K. Powell,[‡,‖] and Ulrich Kortz*[,†]

[†]School of Engineering and Science, Jacobs University, P.O. Box 750 561, 28725 Bremen, Germany

[‡]Institute of Nanotechnology (INT), Karlsruhe Institute of Technology (KIT), Hermann-von-Helmholtz-Platz, 76344, Eggenstein-Leopoldshafen, Germany

[‖]Institute of Inorganic Chemistry, Karlsruhe Institute of Technology (KIT), Engesserstrasse 15, D-76131, Karlsruhe, Germany

[⊥]Key Laboratory of Green Process and Engineering, Institute of Process Engineering, Chinese Academy of Science, 100190, Beijing, China

[#]University of Chinese Academy of Sciences, 100049, Beijing, China

[▽]Laboratoire de Chimie Physique, Groupe d'Electrochimie et de Photoélectrochimie, UMR 8000, CNRS, Université Paris-Sud, Bâtiment 350, 91405 Orsay cedex, France

[⊗]Department of Chemistry, School of Life Sciences, University of Sussex, Brighton BN1 9QJ, United Kingdom

◆Institute for Interdisciplinary Research, Jianghan University, 430056, Wuhan, Hubei, China

**ABSTRACT:** Interaction of the trilacunary Keggin polyanions $[A\text{-}\alpha\text{-}XW_9O_{34}]^{10-}$ (X = $Si^{IV}$, $Ge^{IV}$) with $Co^{II}$ and phosphate ions in aqueous, basic media and under mild heating leads to the formation of the tetrameric, $Co_{16}$-containing heteropolytungstates $[\{Co_4(OH)_3PO_4\}_4(A\text{-}\alpha\text{-}XW_9O_{34})_4]^{32-}$ (X = $Si^{IV}$, $Ge^{IV}$). Both polyanions were characterized in the solid state by single-crystal X-ray diffraction, IR spectroscopy, and thermogravimetric and elemental analyses. Furthermore, the electrochemical and magnetic properties of these isostructural polyanions were investigated.

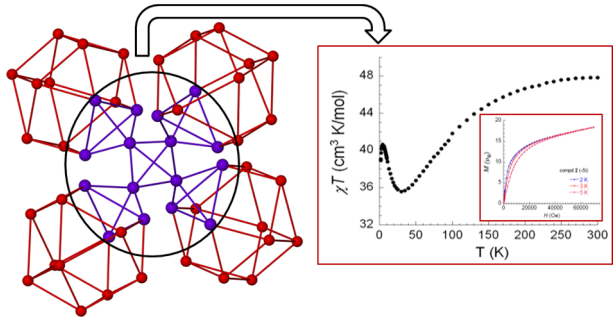


## INTRODUCTION

Polyoxometalates (POMs) have nowadays acquired a significant place in the field of inorganic chemistry due to their evolving structural diversity and applicability in various fields such as catalysis, analytical chemistry, magnetism, nanotechnology, and medicine.[1] Furthermore, lacunary (vacant) heteropolytungstates are known to act as all-inorganic, diamagnetic ligands for various transition metal ions.[1,2] In particular, trilacunary polyanions have a high tendency to stabilize cationic, multinuclear metal-oxo assemblies, leading to compounds with interesting and unusual electronic and magnetic behavior.[2] POM formation in aqueous solution is highly dependent on different variables such as pH, temperature, concentration, reaction medium, and counterions.[3] The chemistry of POMs continues to attract more and more researchers around the world, trying to shed more light on the formation mechanisms, which are still not well understood in general, and often described as self-assembly.

Recently, much attention has been paid to the synthesis of 3d transition metal−oxo assemblies stabilized by lacunary POMs, due to their potential in catalysis and magnetism. In particular, an overview of magnetic transition metal-containing heteropolytungstates has been compiled in two recent reviews.[4] Some examples of multinuclear ($n$ > 6) manganese- and nickel-containing heteropolytungstates are $\{Mn_{10}W_{36}Si_4\}$,[5] $\{Mn_7W_{36}Si_4\}$,[5] $\{Mn_8P_8W_{48}\}$,[6] $\{[Mn^{IV}_2Mn^{III}_6Mn^{II}_4Si_2W_{12}\}$,[7] $\{Ni_7W_{18}P_2(Ale)_2\}$,[8] $\{Ni_7W_{18}P_2(AleNapht)_2\}$,[8] $\{Ni_7W_{18}P_2(AlePy_2)_2\}$,[8] $\{Ni_7W_{18}P_2(AleAc_2)_2\}$,[8] $\{Ni_8Si_2W_{18}L_3\}$ (L = $C_6H_8O_4$, $C_{10}H_8O_4$),[9] $\{Ni_7W_{18}P_2(HAle)_2\}$,[10] $\{Ni_{11}P_2W_{18}(IDA)_3(en)_2(Hen)_2\}$,[11] and $\{Ni_{14}P_{12}W_{60}\}$.[12]

Transition metal-substituted POMs constitute the largest subclass of polyanions, and hence $Co^{II}$-containing heteropolyanions have been intensively investigated, resulting in a large number of structures. The chemistry of cobalt-containing POMs was pioneered in 1956 by Baker. The preparation of two very closely related compounds was reported, with the proposed formulas "$[Co^{II}Co^{II}W_{12}O_{42}]^{8-}$" and

"$[Co^{II}Co^{III}W_{12}O_{42}]^{7-}$".[13] However, in 1966, Baker and Pope showed that these dicobalt derivatives were actually species wherein $Co^{II}$ had replaced a W atom in a Keggin structure, and were then reformulated as $[Co^{II}(H_2O)(Co^{II}W_{11}O_{39})]^{8-}$ and $[Co^{II}(H_2O)(Co^{III}W_{11}O_{39})]^{7-}$.[13b] Later on, magnetic studies were carried out on these compounds.[13c] Since then, much research has been performed in order to explore the chemistry of cobalt-containing POMs. A large number of dimeric, sandwich-type POMs with 2−4 $Co^{II}$ centers encapsulated by lacunary Keggin and Wells−Dawson units have been reported.[14] The pentanuclear Tourné-type sandwich structure $\{Co_3WCo_2W_{18}\}$ comprises tetrahedral and octahedral sites for the $Co^{II}$ centers.[14j,15] The hexanuclear $\{Co_6P_3W_{24}\}$,[16] $\{Co_6V_2W_{24}\}$,[17] and $\{Co^{II}{}_2Co^{III}{}_4Si_2W_{18}(Ac)\}$,[18] as well as the heptanuclear $\{Co_7P_2W_{25}\}$[19] polyanions have also been reported. The octanuclear, carbonate-bridged $\{Co_8Si_2W_{18}O_{34}(CO_3)_3\}$ along with four other $Co^{II}$-containing tungstosilicate complexes have been recently reported by Mialane's group.[20] The nonanuclear trimer $\{Co_9P_5W_{27}\}$, which was first identified as a byproduct by Weakley in 1984,[21] was then fully characterized by Coronado in 1994 including magnetic studies.[2a] Recently, Cronin's group has reported the Wells−Dawson analogue $\{Co_9P_8W_{45}\}$ and also the tetrameric $\{Co_{14}P_{10}W_{60}\}$.[22]

Our group has also been working extensively on the interaction of transition metal ions with lacunary POM precursors.[3e,f,23] In particular for $Co^{II}$, we have reported several compounds covering a range of structures and compositions.[3c,23g,24] Recently, we also reported the largest cobalt aggregate in polyoxotungstate chemistry, $[\{Co_4(OH)_3PO_4\}_4(A\text{-}\alpha\text{-}PW_9O_{34})_4]^{28-}$, which exhibits single-molecule magnet (SMM) behavior, *vide infra*.[23f]

Multinuclear clusters of magnetic ions with large spins and large magnetic anisotropy exhibiting ferromagnetic exchange coupling might also possess SMM behavior. The observation of slow relaxation of magnetization in such metal clusters is of great interest, due to their potential applications in high-density information storage and quantum computation at the molecular level.[25] The first and probably most studied member of the SMMs remains to date the mixed-valence manganese-12 complex $[Mn_{12}O_{12}(OAc)_{16}(H_2O)_4]\cdot 2HOAc\cdot 4H_2O$, commonly known as "$Mn_{12}$-acetate".[26] On the other hand, the field of cobalt(II) SMMs is relatively new, as only a few SMMs of Co(II) have been reported to date. The first $Co^{II}$-based SMM was reported in 2002,[27] which jump-started this area, and meanwhile some more examples have been published.[28] POMs have also contributed to this area, as shown above, and several POM-based SMMs have been reported recently.[23f,29,30]

As part of our ongoing effort to synthesize heteropolytungstates containing high-nuclearity transition metal clusters for magnetic and catalytic purposes, we recently reported the synthesis, structural characterization, and magnetic properties of the 16-cobalt(II) containing 36-tungsto-8-phosphate $[\{Co_4(OH)_3PO_4\}_4(A\text{-}\alpha\text{-}PW_9O_{34})_4]^{28-}$ (**1**). Polyanion **1** represents to date the POM with the highest nuclearity cobalt(II) aggregate and also exhibits SMM behavior.[23f] Wheel-type POM structures containing a total of 16 cobalt(II) centers in the form of four tetramers are also known, but here the tetracobalt assemblies are isolated from each other.[31] To date, there are only a few reports on systematic comparative magnetic and/or electrochemical studies of isostructural polyanions, where only the heteroatom is substituted.[32]

In order to examine a possible influence of the heteroatoms X (X = $P^V$, $Si^{IV}$, $Ge^{IV}$) on the magnetic exchange and redox properties of the central $\{Co_{16}\}$ unit in $[\{Co_4(OH)_3PO_4\}_4(A\text{-}\alpha\text{-}XW_9O_{34})_4]^{n-}$, the synthesis of the germanium and silicon derivatives of **1** is of interest.

## EXPERIMENTAL SECTION

**Reagents and Materials.** The precursor salts $Na_{10}[A\text{-}\alpha\text{-}SiW_9O_{34}]\cdot 23H_2O$ and $Na_{10}[A\text{-}\alpha\text{-}GeW_9O_{34}]\cdot 18H_2O$ were prepared according to the published procedure and characterized by IR spectroscopy.[33] All other reagents were used as purchased without further purification.

**Synthesis of $Na_{32}[\{Co_4(OH)_3PO_4\}_4(A\text{-}\alpha\text{-}SiW_9O_{34})_4]\cdot 78H_2O$ (Na-2).** To a solution of $CoCl_2\cdot 6H_2O$ (0.15 g, 0.63 mmol) in 25 mL of $H_2O$ was added 0.50 g (0.17 mmol) of $Na_{10}[A\text{-}\alpha\text{-}SiW_9O_{34}]\cdot 23H_2O$, and the mixture was stirred until a cloudy pink solution was obtained. The pH of the mixture was then raised to 8 by adding 0.10 g (0.61 mmol) of solid $Na_3PO_4$, and the mixture was stirred for 1 h at room temperature. The clear purple solution obtained after 1 h was then filtered, and the filtrate was allowed to evaporate in an open vial at room temperature. After about a week a purple crystalline product appeared, which was collected then by filtration and air-dried. Yield: 140 mg (27%). IR (2% KBr pellet, $\nu$/cm $^{1}$): 3461 (s), 1627 (s), 1090 (m), 988 (w), 932 (m) 798 (m), 676 (w), 590, 523 (w) (Figure S1 in the Supporting Information). Elemental analysis (%) for $Na_{32}[\{Co_4(OH)_3PO_4\}_4(A\text{-}\alpha\text{-}SiW_9O_{34})_4]\cdot 78H_2O$, calculated (found): Na 5.85 (5.90), P 1.0 (1.0), Co 7.50 (7.53), W 52.6 (52.0), Si 0.89 (0.86).

**Synthesis of $Na_{30.5}K_{1.5}[\{Co_4(OH)_3PO_4\}_4(A\text{-}\alpha\text{-}GeW_9O_{34})_4]\cdot 116H_2O$ (KNa-3).** $CoCl_2\cdot 6H_2O$ (0.12 g, 0.50 mmol) was dissolved in 20 mL of $H_2O$. Then $Na_{10}[A\text{-}\alpha\text{-}GeW_9O_{34}]\cdot 18H_2O$ (0.50 g, 0.18 mmol) was added, and the mixture was stirred until a clear, purple solution was obtained. The pH of the solution was maintained at 8 with 4 M $KOH_{(aq)}$ and stirring continued for 30 min at room temperature. Then 0.50 g (3.1 mmol) of $Na_3PO_4$ was added in small portions while the pH was maintained at 8.0−8.5 with $HCl_{aq}$. The resulting turbid solution was stirred for 1 h at 75 °C and became clear during heating. The solution was allowed to cool to room temperature and then filtered. The clear, purple filtrate was kept in an open vial at room temperature for slow evaporation. After 1 day a purple crystalline product started to appear, which was collected after 2 days by filtration and air-dried. Yield: 120 mg (19%). IR (2% KBr pellet, $\nu$/cm $^{1}$): 3460 (s), 1631 (s), 1094 (m), 926 (m), 816 (m), 672 (w), 590 (w), 518 (w) (Figure S1 in the Supporting Information). Elemental analysis (%) for $Na_{30.5}K_{1.5}[\{Co_4(OH)_3PO_4\}_4(A\text{-}\alpha\text{-}GeW_9O_{34})_4]\cdot 97H_2O$, calculated (found): Na 5.34 (5.53), K 0.45 (0.46), P 0.94 (1.01), Co 7.19 (7.34), W 50.5 (48.3), Ge 2.19 (2.21).

**IR, TGA, and Elemental Analysis.** Infrared spectra were recorded on a Nicolet Avatar 370 FT-IR spectrophotometer using KBr pellets (Figure S1 in the Supporting Information). The following abbreviations were used to assign the peak intensities: w = weak, m = medium, and s = strong. Thermogravimetric analyses were carried out on a TA Instruments SDT Q600 thermobalance with a 100 mL/min flow of nitrogen; the temperature was ramped from room temperature to 500 °C at a rate of 5 °C/min (Figures S2 and S3 in the Supporting Information). Elemental analyses for **Na-2** and **KNa-3** were performed by CNRS, Service Central d'Analyze, Solaize, France.

**X-ray Crystallography.** Each crystal was mounted on a Hampton cryoloop in light oil for data collection at −173 °C. Indexing and data collection were performed on a Bruker D8 SMART APEX II CCD diffractometer with kappa geometry and Mo K$\alpha$ radiation (graphite monochromator, $\lambda$ = 0.71073 Å). Data integration was performed using SAINT.[34] Routine Lorentz and polarization corrections were applied. Multiscan absorption corrections were performed using SADABS.[35] Direct methods (SHELXS97) successfully located the tungsten atoms, and successive Fourier syntheses (SHELXL97/2013) revealed the remaining atoms.[36] Refinements were full-matrix least-squares against $|F^2|$ using all data. In the final refinement, all nondisordered heavy atoms (Na, K, Co, Si, Ge, W) were refined anisotropically; oxygen atoms and disordered countercations were

**Table 1. Crystal data for Na-2 and KNa-3**

| | Na-2 | KNa-3 |
|---|---|---|
| empirical formula | $H_{168}Co_{16}Na_{32}O_{242}P_4Si_4W_{36}$ | $H_{244}Co_{16}Ge_4K_{1.50}Na_{30.50}O_{280}P_4W_{36}$ |
| formula weight, g/mol | 12574.75 | 13461.50 |
| crystal system | rhombohedral | cubic |
| space group | $R\bar{3}$ | $Fd\bar{3}$ |
| $a$, Å | 24.8510(6) | 35.5650(9) |
| $b$, Å | 24.8510(6) | 35.5650(9) |
| $c$, Å | 60.8811(12) | 35.5650(9) |
| $\alpha$, deg | 90.00 | 90.00 |
| $\beta$, deg | 90.00 | 90.00 |
| $\gamma$, deg | 120.00 | 90.00 |
| vol, Å$^3$ | 32561.2(13) | 44985(3) |
| $Z$ | 6 | 8 |
| $D_{calc}$, g/cm$^3$ | 3.848 | 3.975 |
| abs coeff | 20.423 | 20.261 |
| $F(000)$ | 34 008 | 49 056 |
| cryst size, mm | 0.40 × 0.35 × 0.06 | 0.34 × 0.26 × 0.20 |
| theta range for data collection, deg | 3.43−21.96 | 3.44−30.5 |
| reflns collected | 174 269 | 151 051 |
| indep reflns | 8821 | 5740 |
| $R$(int) | 0.1427 | 0.1020 |
| obsd ($I > 2\sigma(I)$) | 6472 | 3890 |
| goodness-of-fit on $F^2$ | 1.0003 | 1.004 |
| R1 [$I > 2\sigma(I)$]$^a$ | 0.0934 | 0.0733 |
| wR2 (all data)$^b$ | 0.2860 | 0.2433 |

$^a R = \sum||F_o| - |F_c||/\sum|F_o|$. $^b R_w = [\sum w(F_o^2 - F_c^2)^2/\sum w(F_o^2)^2]^{1/2}$.

refined isotropically. No hydrogen atoms were included in the models. For **Na-2**, the crystal diffracted only to low theta(max), most likely due to the high degree of disorder of countercations and crystal waters. For **KNa-3** the 1.5 potassium countercations were not found by single crystal XRD, but rather by elemental analysis. Nevertheless, for overall consistency, the formula based on elemental analysis, representing the composition of the bulk material, is used throughout this paper, also in the crystallographic files. Crystallographic data are summarized in Table 1.

**Electrochemical Measurements.** The electrochemical setup was an EG & G 273 A driven by a PC with the M270 software or a CHI660E driven by a PC with the CHI software. Potentials are quoted against a saturated calomel electrode (SCE). The counter electrode was a platinum gauze of large surface area. All experiments were performed at room temperature. The source, mounting, and polishing of the glassy carbon[37] or ITO electrodes have been described.[23e] Controlled-potential coulometry experiments were carried out with a large surface area carbon plate. The solutions were deaerated thoroughly for at least 30 min with pure argon and kept under a positive pressure of this gas during the experiments. The solutions were 10 $^{4}$ M in POM. The composition of the aqueous electrolyte was 1 M $CH_3COOLi$ + $CH_3COOH$ (pH 7). The electrochemical experiments were performed in the dark. UV−vis spectra were recorded with a Lambda 750 PerkinElmer spectrophotometer. The solutions were placed in quartz cuvettes with an optical path of 0.2 or 0.1 cm.

**Magnetic Suseptibility Measurements.** Magnetic susceptibility measurements (1.8−300 K) were obtained with a Quantum Design SQUID magnetometer MPMS-XL. This magnetometer works between 1.8 and 400 K for dc applied fields ranging from −7 to 7 T. The SQUID measurements were performed on polycrystalline samples of **Na-2** and **KNa-3**. Alternating current (ac) susceptibility measurements were performed for both compounds with an oscillating ac field of 3 Oe and ac frequencies ranging from 1 to 1500 Hz. $M$ versus $H$ measurements were performed at 100 K to check for the presence of ferromagnetic impurities; none were observed. The magnetic data were corrected for the sample holder and the diamagnetic contribution.

## RESULTS AND DISCUSSION

**Synthesis and Structure.** Polyanions **2** and **3** were synthesized in simple one-pot reactions of $CoCl_2{\cdot}6H_2O$ with $Na_{10}[A\text{-}\alpha\text{-}SiW_9O_{34}]{\cdot}23H_2O$ and $Na_{10}[A\text{-}\alpha\text{-}GeW_9O_{34}]{\cdot}18H_2O$, respectively, in aqueous medium at pH 8 in the presence of phosphate ions, and then isolated as hydrated sodium salts, $Na_{32}[\{Co_4(OH)_3PO_4\}_4(A\text{-}\alpha\text{-}SiW_9O_{34})_4]{\cdot}78H_2O$ (**Na-2**) and $Na_{30.5}K_{1.5}[\{Co_4(OH)_3PO_4\}_4(A\text{-}\alpha\text{-}GeW_9O_{34})_4]{\cdot}116H_2O$ (**KNa-3**), respectively. Single crystal X-ray diffraction analyses on these salts revealed that polyanions **2** and **3** are isostructural; therefore, only the structure of **2** is described in detail here. Polyanion **2** is composed of four tri-$Co^{II}$-substituted Keggin units, $\{(A\text{-}\alpha\text{-}SiW_9O_{34})(CoOH)_3\}$, connected by four $\{PO_4\}$ linkers and encapsulating a central $\{Co_4O_4\}$ cubane fragment in a tetrameric fashion with idealized $T_d$ point group symmetry. The structure of polyanion **2** can also be viewed as a tetrahedral assembly with a central $[Co_4(PO_4)_4]^{4-}$ core surrounded by four $\{(A\text{-}\alpha\text{-}SiW_9O_{34})(CoOH)_3\}$ units at the four vertices (Figure 1). As shown in Figure 2, the central $[Co_{16}(OH)_{12}(PO_4)_4]^{8+}$ fragment consists of four triangular $\{Co_3(OH)_3\}$ fragments, four $\{PO_4\}$ linkers, and a central $\{Co_4O_4\}$ cubane core. Each $Co^{II}$ center in the cubane unit is coordinated by three $\mu_3$-OH groups belonging to $[(A\text{-}\alpha\text{-}SiW_9O_{34})(CoOH)_3]^{7-}$ units and a $\mu_4$-oxygen atom of the three $\{PO_4\}$ linkers. Each of the four phosphate groups links three $[(A\text{-}\alpha\text{-}SiW_9O_{34})(CoOH)_3]^{7-}$ fragments via three $P{-}O_{(Co)}$ bonds, one to each Keggin fragment.

All the $Co^{II}$ centers in the $[Co_{16}(OH)_{12}(PO_4)_4]^{8+}$ fragment exhibit a distorted $\{CoO_6\}$ octahedral geometry, and all the $\{PO_4\}$ linkers show a tetrahedral geometry. The Co−O bond lengths and O−Co−O bond angles are in the range of 2.00(3)−2.38(3) Å and 72.9(11)−172.6(13)°, respectively (see Table S1 in the Supporting Information). For **3** the Co−O

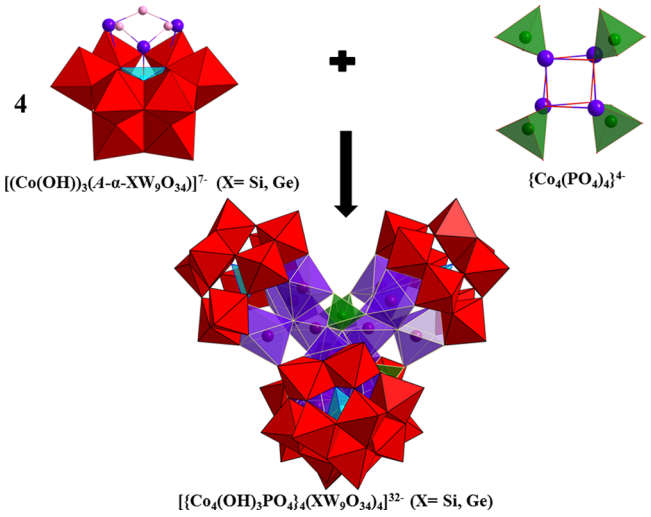


**Figure 1.** Combined polyhedral/ball-and-stick representation of the various building blocks comprising polyanions **2** and **3**. Color code: $WO_6$ red octahedra, $CoO_6$ violet octahedra, $PO_4$ green tetrahedra, $XO_4$ blue tetrahedral (X = Si, Ge), Co violet balls, O red balls. Protonated oxygens are shown in lavender.

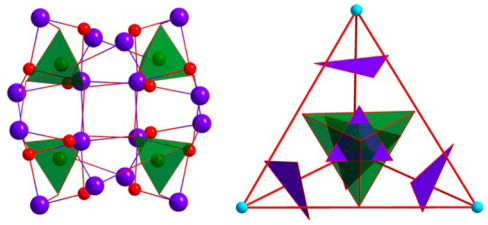

**Figure 2.** Left: Ball-and-stick representation of the $[Co_{16}(OH)_{12}(PO_4)_4]^{8+}$ core in **2** and **3**. Right: Representation of the various tetrahedral building units in **2** and **3** formed by connection of the four X heteroatoms, the four capping P atoms, the four central Co atoms, and the four triangular $Co_3$ groups. The color code is the same as in Figure 1.

bond lengths and O−Co−O bond angles are in the ranges 2.063(11)−2.226(13) Å and 81.0(6)−167.5(3)°, respectively.

Protonated oxygens of the polyanions were located by bond valence sum (BVS) calculations.[38] All $\mu_3$-oxo$_{(Co)}$ bridges in polyanions **2** and **3** are monoprotonated, adding up to 12 for each polyanion, and all phosphate oxygens are nonprotonated, leading to the general formula $[\{Co_4(OH)_3PO_4\}_4(A\text{-}\alpha\text{-}XW_9O_{34})_4]^{32-}$ (X = Si, **2**; Ge, **3**). The total charge is balanced in the solid state by 32 sodium countercations in **Na-2**, and by 30.5 sodium and 1.5 potassium countercations in **KNa-3** (the source of potassium ions being the potassium hydroxide solution used for pH adjustment). For both compounds the complete composition including countercations and crystal waters was determined by elemental analysis (see Experimental Section), and we also confirmed the number of crystal waters by thermogravimetric analysis (TGA, see Figures S2 and S3 in the Supporting Information). Based on both techniques, elemental analysis and TGA, 78 crystal waters for **Na-2** and 116 crystal waters for **KNa-3** were included in the final formula units.

Both polyanions **2** and **3** were synthesized in slightly basic (pH 8) aqueous medium and with mild heating, and in both cases the presence of phosphate ions was required. The presence and possible template effect of small anions including phosphate in POM synthesis are well-known, and several examples have been reported.[2b,k,39] The silicon analogue **2** crystallized as a sodium salt **Na-2** in the rhombohedral space group $R\bar{3}$, whereas the germanium analogue **3** crystallized in the cubic space group $Fd\bar{3}$. The optimized synthesis of polyanion **2** required only one step, whereas the germanium analogue **3** was synthesized in a slightly modified, two-step procedure, as this led to a higher yield and also better quality crystals for single crystal X-ray diffraction. The important first step for the synthesis of **3** involves maintaining the pH value to 8 by addition of potassium hydroxide. For the synthesis of **2** the sequence of adding the reagents was of importance, as otherwise the desired product could not be obtained. For example, if the cobalt(II) salt is added to the aqueous sodium phosphate solution (pH 8), a large amount of purple precipitate (most probably cobalt phosphate) is formed, leaving a colorless supernatant. Moreover, if the Keggin precursor was added before the $Co^{II}$ ions, the resultant mixture was turbid and gave a purple colored filtrate, which produced a purple precipitate with a different FT-IR spectrum compared to **Na-2**. We discovered that polyanion **3** could be obtained in higher yield when more sodium phosphate was added during the synthesis. Also, the presence of potassium ions from $KOH_{(aq)}$ was crucial in order to form bulk-pure crystalline **KNa-3**. The above indicates a slightly different chemical reactivity of the trilacunary POM precursors $[A\text{-}\alpha\text{-}SiW_9O_{34}]^{10-}$ and $[A\text{-}\alpha\text{-}GeW_9O_{34}]^{10-}$ in our reaction system.

**Topological Features.** In recent years a novel method for the description of high nuclearity clusters has been established[40] and developed.[41] This methodology is based on considering each metal center as a node and every monatomic bridge (O, N, S) as a linker resulting in a decorated motif. The resulting graph of each polynuclear compound can be described by a unique *NDk-m* symbol,[42] where *N* is the set of coordination numbers of topologically nonequivalent nodes, *D* is dimensionality; *D* = *M* for finite (molecular) clusters, *k* is the number of nodes in the cluster, and *m* enumerates topologically different clusters with the same *NDk* symbol. An isolated metal atom is designated (0). Thus, every *NDk-m* symbol denotes a topological type, i.e., a set of topologically equivalent but likely conformationally different CC skeletons.

This approach can be used to (a) easily identify structural similarities,[43] (b) find all the compounds of the some nuclearity, and (c) compare the decorated motifs through the subgraph search.[44] This methodology has been successfully applied in compounds which contain organic ligands and solely Mn centers (539 compounds),[41,45] Co centers (312 compounds),[46] and Ni centers (318 compounds).[47]

Interestingly, this approach can be successfully applied in POM chemistry, where inorganic subunits are linked together in various ways. However, it is worth stating that in POM chemistry there is a need for classifying all inorganic subunits as well the entire polyanion, in order to utilize these motifs in future searches. The application of this approach to POMs may give the opportunity, after classifying a plethora of compounds, to identify, through subgraph search, compounds with structural similarities as well to create libraries for each inorganic subunit. Moreover, this approach offers an alternative way of presenting these gigantic but aesthetically pleasing anions.

In this context, excluding the countercations from the simplification process, polyanions **1**−**3** can be described as a motif enumerated as **4,4,5,6M52-1** (Figure 3). Finally, the

central $\{Co_{16}\}$ unit can be described as **3,6M16-1** (Figure 4), and a literature survey in the Co library[46] shows that such motif is so far unknown in Co chemistry.

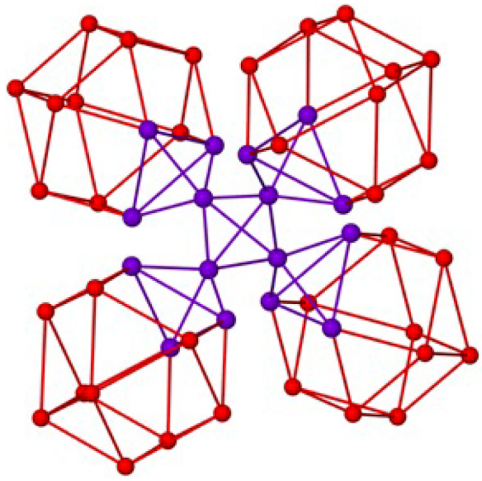

**Figure 3.** The decorated motif 4,4,5,6M52-1 of polyanions **1**−**3**. Color code: W (red balls), Co (violet balls).

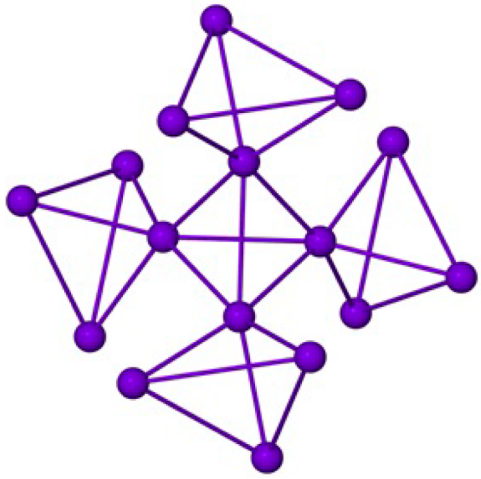

**Figure 4.** The decorated motif 3,6M16-1 of the $\{Co_{16}\}$ core in **1**−**3**. Color code: Co (violet balls).

**Magnetic Studies.** The magnetic properties of polyanions **2** and **3** were investigated using polycrystalline samples dispersed in Apiezon grease. Such studies also allow for a comparison with the isostructural analogue **1**, and to examine the effect of the heteroatoms (P vs Si vs Ge) on the overall magnetic properties. The magnetic plots are shown in Figures S4 and S5 in the Supporting Information as $\chi T$ vs $T$ and $M$ vs $H$. As expected, both compounds exhibit a very similar temperature dependence of the magnetic susceptibility, in which, upon lowering the temperature, the $\chi T$ value first declines gradually and then increases rapidly to reach a maximum and finally falls sharply until 1.8 K. Such behavior indicates that dominant ferromagnetic interactions are present in both compounds, but the decrease of the $\chi T$ value at high temperatures originates from spin−orbit coupling of the $Co^{II}$ ions. The room temperature $\chi T$ value of 47.81 $cm^3$ K $mol^{-1}$ for **2** and 50.56 $cm^3$ K $mol^{-1}$ for **3** is much higher than the expected one (30.0 $cm^3$ K $mol^{-1}$) for 16 spin-only high-spin $Co^{II}$ ions ($S$ = 3/2, $g$ = 2, $C$ = 1.875 $cm^3$ K $mol^{-1}$) due to a strong orbital contribution of the $Co^{II}$ ions. The final decrease below 5 K is associated with magnetic anisotropy, as all the $Co^{II}$ ions are shielded by the diamagnetic POM shells, thus not allowing for intermolecular antiferromagnetic interactions. It is noticeable that the product $\chi T$ for **2** reaches a maximum of 40.64 $cm^3$ K $mol^{-1}$ at 4.0 K, higher than that of 36.15 $cm^3$ K $mol^{-1}$ at 4.5 K for **3**. In complete agreement with the isostructural analogue **1**,[23f] the 16 $Co^{II}$ ions in **2** and **3** are ferromagnetically coupled, leading to a ground spin state of $S$ = 8, in which the $(\chi T)_{max}$ should reach about 48.24 $cm^3$ K $mol^{-1}$ with $g$ = 2.3. The lower $(\chi T)_{max}$ observed for **2** and **3**, as compared to **1**, result in $g$ = 2.13 and 2.0, respectively, both also lower than for **1**. The electronic configuration and ionic radius resulting from the outermost shell of different heteroatoms influence how compact the tetrahedral $\{Co_4(PO_4)_4\}^{4-}$ cores packed in the lattice. This is evidenced in the Co−O bond lengths and O−Co−O bond angles, which are slightly different from compound **2** to **3**, as described in the structural part. Therefore, the most likely reason for these slight differences between the three isostructural compounds is that, depending on the different heteroatoms (P vs Si vs Ge) in the respective POM unit, weak antiferromagnetic interactions mediated within the tetrahedral $\{Co_4(PO_4)_4\}^{4-}$ cores appear to become significant, compared to the overall ferromagnetic coupling. However, the differences are small; the magnetic properties of the system do indeed appear to be robust overall, being largely independent of the type of trilacunary POM precursor used. Furthermore, the dominance of ferromagnetic interactions in **2** and **3** is further confirmed by the field dependence of the magnetization at low temperatures, in which the magnetization increases very fast with a small external field, but without saturation even up to 70 kOe (Figure S5 in the Supporting Information).

The dynamic properties of compounds **2** and **3** also show similar behavior as **1**. The temperature dependence of both in-phase and out-of-phase components are frequency dependent, indicating the presence of slow magnetic relaxation. The shape and frequency dependence of the ac magnetic susceptibility both suggest that these two compounds behave as SMMs (Figures 5 and 6). The relaxation time can be deduced from the frequency sweeping ac data. In both cases, the data between 1.8 and 2.8 K follow a thermally activated behavior with an energy gap ($\Delta$) of 24.8 K and a pre-exponential factor ($\tau_0$) of $1.6 \times 10^{-8}$ s for **2**, as well as 25.9 K and $1.2 \times 10^{-8}$ s for **3** (Figure S6 in the Supporting Information). The set of characteristic parameters observed for these two compounds is very similar, and is also comparable to the isostructural analogue **1**.[23f] The similar SMM behavior observed for all these three compounds further suggests that their overall magnetic properties are largely independent of the heteroatoms used in the trilacunary POM precursor. Furthermore, the ac measurements under an applied dc field were performed on both compounds to study the relaxation behavior further and to check for quantum tunneling effects above 1.8 K. However, application of a dc field did not influence significantly the relaxation process of these compounds, indicating that the quantum tunneling effect in this system is not very pronounced (Figures S7 and S8 in the Supporting Information).

**UV−Visible Absorption Spectroscopy.** The UV−visible absorption spectra of **2** and **3** in a pH 7 acetate medium are shown in Figure S9 in the Supporting Information. In the UV region, the spectra exhibit intense absorption bands around 246 nm (the $\lambda_{max}$ are ca. $1.38 \times 10^5$ $M^{-1}$ $cm^{-1}$ for **2** and $1.16 \times 10^5$

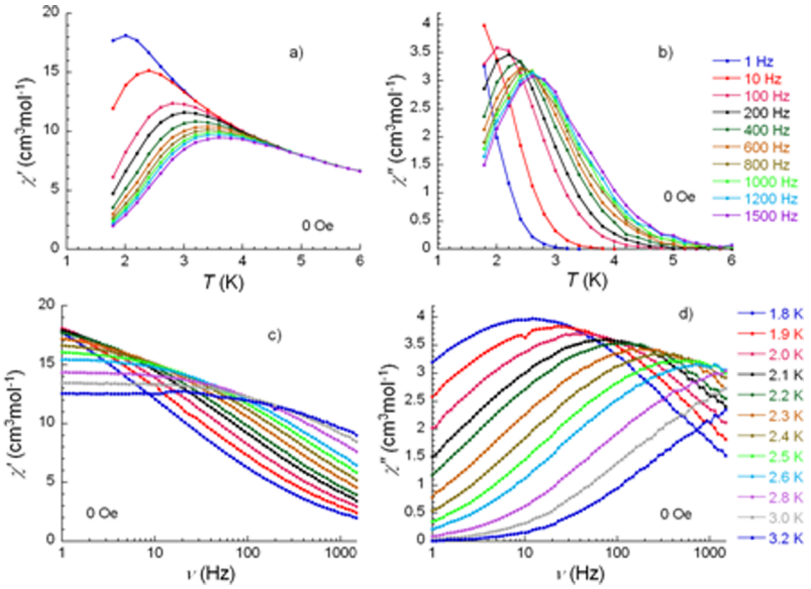


**Figure 5.** Temperature dependence of the in-phase (a) and out-of-phase (b) components of the ac magnetic susceptibility at different frequencies and frequency dependence of the in-phase (c) and the out-of-phase (d) components of the ac susceptibility at different temperatures for **2** under zero dc field.

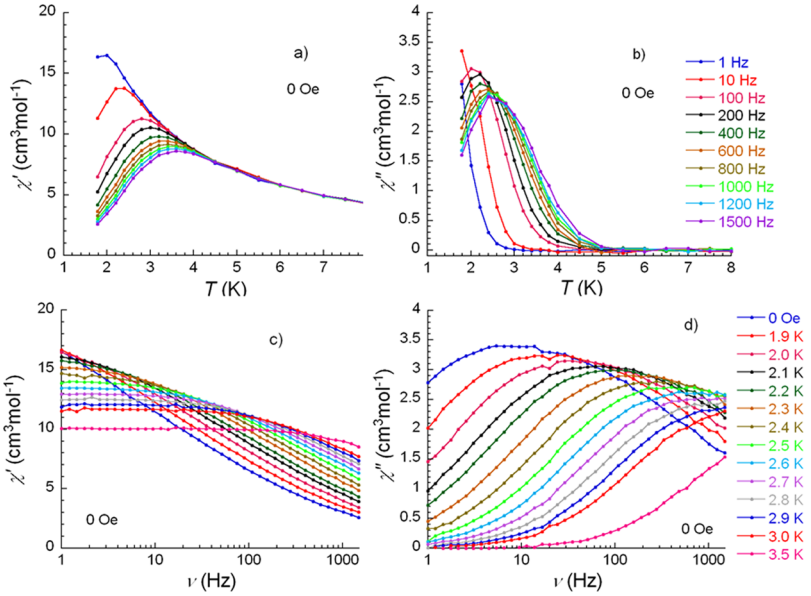


**Figure 6.** Temperature dependence of the in-phase (a) and out-of-phase (b) components of the ac magnetic susceptibility at different frequencies and frequency dependence of the in-phase (c) and the out-of-phase (d) components of the ac susceptibility at different temperatures for **3** under zero dc field.

$M^{-1}$ $cm^{-1}$ for **3**). These absorption bands are due to oxygen-to-tungsten charge transfer transitions. As expected, the spectra of the cobalt centers present several absorption bands in the visible light region (Figure S9B in the Supporting Information).[20] The characteristics of these Co bands feature distinct fingerprints of the two POMs. Thus, the spectrum of **2** exhibits a broad band roughly at 530 nm followed by two peaks at 512 nm ($\varepsilon_{max}$ ca. 470 $M^{-1}$ $cm^{-1}$) and 484 nm ($\varepsilon_{max}$ ca. 466 $M^{-1}$ $cm^{-1}$), whereas that of **3** is characterized by a peak at 538 nm ($\varepsilon_{max}$ ca. 437 $M^{-1}$ $cm^{-1}$) followed by two shoulders at ca. 512 and 490 nm, respectively.

**Electrochemical Studies.** The electrochemical behavior of **2** and **3** was studied in an aqueous pH 7 acetate medium. For this purpose, the stabilities of the compounds in this medium were assessed by monitoring their respective UV−visible spectra. A complementary cross-check of this stability was obtained by cyclic voltammetry (CV). The two compounds were stable enough in this medium for their CV characterization. The study is restricted to the waves for which no derivatization of the electrode was observed.[48] Moreover, the irreversible waves associated with the $W^{VI}$ reduction or $Co^{II}$ oxidation processes will not be studied here. These processes are featured by waves located close to the electrolyte reduction or oxidation. For clarity, the redox processes associated with the $Co^{II}$ and $W^{VI}$ centers are described separately.

Figure 7 shows the superimposed CV patterns of **2** and **3** restricted to their first quasi-reversible W-waves. In agreement with expectations from previous works,[32e,49] the reduction of

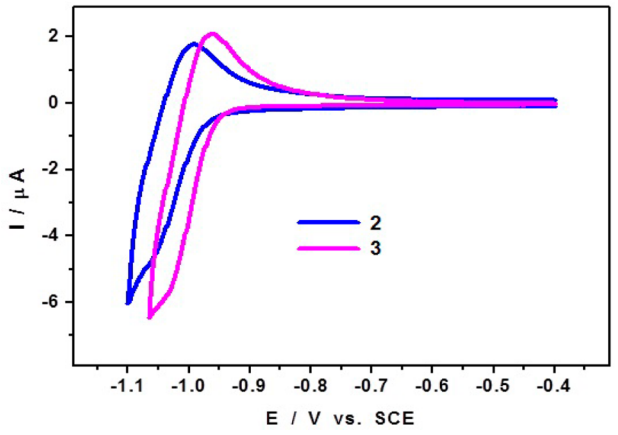


**Figure 7.** Cyclic voltammograms of the first $W^{VI}$-waves of **2** and **3**, respectively, run in a pH 7 (1 M $CH_3COOLi$ + $CH_3COOH$) medium; the scan rate was 10 mV $s^{-1}$, and the reference electrode was a saturated calomel electrode (SCE). The concentration of the polyanions was $10^{-4}$ M.

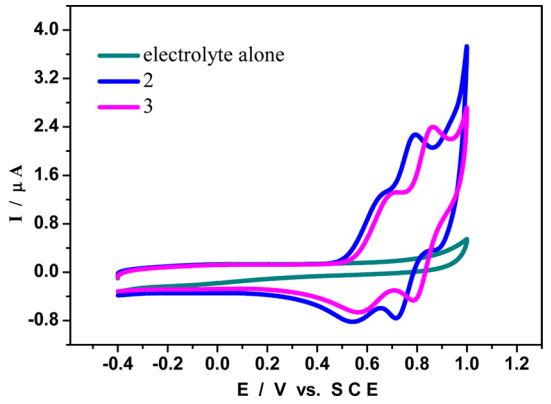


**Figure 8.** Comparison of the cyclic voltammograms of $10^{-4}$ M of **2** and **3** in a pH 7 (1 M $CH_3COOLi$ + $CH_3COOH$) medium and that of the corresponding background current. The scan rate was 10 mV $s^{-1}$, and the reference electrode was a saturated calomel electrode (SCE). The CV patterns feature the redox processes associated with the $Co^{II}$ centers.

the $W^{VI}$ centers in the Ge derivative **3** are slightly easier than those of the Si derivative **2**. In other words, the $W^{VI}$ centers reduction waves associated with **2** are cathodically shifted with respect to those of **3**. Both complexes present also a large intensity wave which is the combination of their irreversible multielectronic reduction and the electrolyte reduction wave. Indeed, as an irreversible electrode derivatization proceeds in this potential domain, the potential location of such reduction waves and that of the electrolyte vary with the number of cycles.[48] Such complex phenomena will not be considered in the following. The formal potentials $E^0$, calculated as the average between the cathodic and anodic peak potentials, are ca. −1.04 V for **2** and −1.00 V vs SCE for **3**. As a consequence, the first redox couple of **2** is very close to the electrolyte reduction limit (onset potential at ca. −1.180 V vs SCE for the very first CV), whereas Figure S10 in the Supporting Information shows that the CV of **3** contains a second W-wave peaking at −1.13 V vs SCE. This demonstrates that the CVs represent a fingerprint for **2** and **3**, similar to those reported for other POMs based on $\{XW_9O_{34}\}$ units.[49c]

In the positive potential domain (vs SCE), the $Co^{II}$ centers in **2** and **3** feature two quasi-reversible oxidation waves with the same general shape (Figure 8). However, when compared to **2**, slight anodic shifts of ca. 0.05 and 0.07 V were observed for the formal potentials of the two quasi-reversible processes associated with **3** (ca. +0.640 and +0.825 V vs SCE respectively). To our knowledge, such observations represent only the third example of electrochemically well-behaved $Co^{II}$ centers in a multi-cobalt-substituted POM. The two other examples were described by Kortz and Mialane, respectively.[20,24b] Moreover, there is no report on such results in a pH 7 medium.

Potential-controlled coulometry was used to establish the actual electron consumption for each oxidation wave of the $Co^{II}$ centers (0.2 mM **2** or **3**). The electrolysis performed on the first oxidation wave of the $Co^{II}$ centers in **3** (at +0.780 V vs SCE) consumes 3.7 electrons per molecule of POM. When the electrolysis was carried out at +0.95 V vs SCE, just beyond the second oxidation peak of the $Co^{II}$ centers, the oxidation process continues even after 25 electrons per molecule, which is ca. 1.56 times the number needed for monoelectronic oxidation of all the $Co^{II}$ centers to $Co^{III}$. This observation is likely due to thin film deposition during the electrolysis. Such a phenomenon is not unprecedented, as previously reported by Kortz and co-workers for $[Co_6(H_2O)_{30}\{Co_9Cl_2(OH)_3(H_2O)_9(\beta\text{-}SiW_8O_{31})_3\}]^{5-}$.[23g] However, we observed that this process is strongly influenced by the type of heteroatom (Si vs Ge) in the lacunary Keggin units of **2** and **3**. Indeed, the oxidation of **2** performed with the potential set at +0.88 V vs SCE (on the second Co-wave) showed a progressive inhibition of the electrode response which prevents a reliable determination of the number of electrons involved in the $Co^{II}$ oxidation by potential-controlled coulometry in this medium. The inhibition of the oxidation process is attributed to the deposition of a poorly conducting film on the electrode surface. Indeed, the CV pattern of **2** obtained with this modified electrode exhibits ill-defined and low intensity waves when compared to the characteristics of that recorded with the bare electrode. In contrast, for **3** the patterns observed with both electrodes are well-defined and a slight cathodic shift of ca. 0.030 V (for the first oxidation wave) is observed for the modified electrode, which means that the oxidation of the $Co^{II}$ centers becomes slightly easier with the modified electrode. The cathodic shift of the second oxidation wave is not significant (ca. 6 mV). However, the overall electron transfer process associated with this redox couple estimated from the anodic-to-cathodic peak potential differences of the second redox couple is slightly faster with the modified electrode ($\Delta Ep_2$ = 0.071 V) than with the bare electrode ($\Delta Ep_2$ = 0.094 V). A similar improvement was also observed for the first redox couple (the $\Delta Ep_1$ values are 0.095 and 0.125 V, respectively, for the modified and the bare electrode). Altogether, these observations show that the modified electrode is more active toward the oxidation of the $Co^{II}$ centers. The beneficial effect of electrode pretreatment by continuous scanning of the potential in relatively high potential was demonstrated by Sadakane in his pioneering work on the oxidation the Mn(II) center within $K_6[Mn(H_2O)SiW_{11}O_{39}]$.[50] The electrochemical behavior observed with the bare electrode was restored by repolishing both modified electrodes, which underscores a modification process occurring during the bulk electrolyses. It is worth noting that, for both POMs, the observed electrode modifications proceed very slowly. Indeed, even for relatively slow scan rates (between 10 and 2 mV $s^{-1}$), the variation of the peak current intensities as a function of the

square root of the potential scan rate indicates that the CVs feature a diffusion-controlled process. Such observations are not unprecedented. For example, Keita and co-workers reported a similar observation for the oxidation of the Mn centers in $[(Mn^{III}(H_2O))_3(SbW_9O_{33})_2]^{9-}$.[51] The electrochemical quartz crystal microbalance (EQCM) used in this work demonstrates that a very thin film deposition process occurs during the generation of the $Mn^{IV}$ state. However, for scan rates between 20 and 100 mV $s^{-1}$, the peak current intensity of the $Mn^{IV}$ oxidation wave varies linearly with the square root of $\nu$, which indicates that the CVs feature a diffusion-controlled process at these scan rates. Moreover, even at slower scan rates (between 20 and 2 mV $s^{-1}$) the oxidation is governed by a mixed adsorption−diffusion regime (a purely adsorption regime was not observed). This phenomenon corresponds probably to the slow formation of a very thin film of $MnO_x$ during the Mn center oxidation. Although we did not perform EQCM for the investigation of the film formation in the current work, we attribute tentatively our observation to a slow thin film formation. Moreover, there are several reports on film formation on the electrode surface during oxidation of Co-POMs.[52]

## CONCLUSIONS

We have synthesized and structurally characterized the 16-cobalt(II)-containing 36-tungsto-4-silicate $[\{Co_4(OH)_3PO_4\}_4(A\text{-}\alpha\text{-}SiW_9O_{34})_4]^{32-}$ (**2**) and the isostructural germanate $[\{Co_4(OH)_3PO_4\}_4(A\text{-}\alpha\text{-}GeW_9O_{34})_4]^{32-}$ (**3**) in a simple, one-pot procedure by reaction of the trilacunary Keggin precursors $[A\text{-}\alpha\text{-}SiW_9O_{34}]^{10-}$ and $[A\text{-}\alpha\text{-}GeW_9O_{34}]^{10-}$, respectively, with $Co^{II}$ and phosphate ions in aqueous medium. Polyanions **2** and **3** are isostructural with their P analogue $[\{Co_4(OH)_3PO_4\}_4(PW_9O_{34})_4]^{28-}$ (**1**) and consist of a cationic $[Co_{16}(OH)_{12}(PO_4)_4]^{8+}$ assembly stabilized by four trilacunary $[A\text{-}\alpha\text{-}SiW_9O_{34}]^{10-}$ and $[A\text{-}\alpha\text{-}GeW_9O_{34}]^{10-}$ units, respectively, resulting in a structure with $T_d$ point group symmetry. The hydrated salts **Na-2** and **KNa-3** were investigated in the solid state by single-crystal XRD, FT-IR spectroscopy, and thermogravimetric and elemental analyses. We have also investigated the electrochemistry of **2** and **3** in aqueous solution. Furthermore, we have studied the magnetic properties of **Na-2** and **KNa-3**, in order to examine the effect of the heteroatoms (Si vs Ge) on the overall magnetic properties, and to compare them with those of the P-analogue **1**. These studies revealed that all three polyanions **1**−**3** are SMMs. Our studies demonstrate that it is worthwhile to try and create isostructural families of compounds, which allow for rationalizing any small changes in physicochemical behavior (e.g., magnetic, electronic, redox) as being due to changes in hetero group, and hence composition and charge of the polyanion. Interestingly, the synthetic conditions of polyanions **2** and **3** are not strictly identical, which emphasizes once again the challenges associated with POM synthesis.

In summary, the synthesis of **2** and **3** (as well as **1**) demonstrates a novel and efficient route for the preparation of high-nuclearity 3d transition metal complexes encapsulated by POM ligands. In recent years we have been systematically developing rational synthetic procedures by using simple transition metal salts and lacunary polyanions, and we discovered that aqueous, basic media are ideal. Based on such a synthetic strategy, we have already succeeded in isolating several more multinuclear 3d metal-containing polyanions, namely, $\{Mn_{16}\}$, $\{Mn_8\}$, $\{Ni_{16}\}$, $\{Ni_{13}\}$, $\{Fe_{14}\}$, and $\{Cu_{15}\}$, which will be reported elsewhere.

## AUTHOR INFORMATION


### Corresponding Author

*E-mail: u.kortz@jacobs-university.de. Fax: +49 421 200 3229. Tel: +49 421 200 3235.

### Present Address

[¶](M.I.) Karlsruhe Institute of Technology (KIT).

### Author Contributions

[§]M.I. and A.H. contributed equally to this work.


### Notes

The authors declare no competing financial interest.

## ACKNOWLEDGMENTS


U.K. thanks the German Science Foundation (DFG, KO 2288/20-1, KO 2288/4-1, KO 2288/3-1, and KO 2288/3-2), the CMST COST Action CM1203 (PoCheMoN), and Jacobs University for research support. M.I. thanks DAAD and Higher Education Commission of Pakistan for a doctoral fellowship. She also thanks the University of Balochistan, Quetta, Pakistan for allowing her to pursue her Ph.D. studies at Jacobs University, Germany. M.I. also thanks Institute of Nanotechnology (INT)-Karlsruhe Institute of Technology (KIT) for the guest scientist fellowship. A.H. thanks DAAD for a doctoral fellowship. Y.L. and A.K.P. acknowledge support from the DFG Center for Functional Nanostructures. Figures 1 and 2 were generated by *Diamond*, Version 3.2 (copyright Crystal Impact GbR).


## REFERENCES


(1) (a) Pope, M. T. *Heteropoly and Isopoly Oxometalates*; Springer: Berlin, 1983. (b) Pope, M. T.; Müller, A. *Angew. Chem., Int. Ed. Engl.* **1991**, *30*, 34−48. (c) Hill, C. L.; Prosser-McCartha, C. M. *Coord. Chem. Rev.* **1995**, *143*, 407−455. (d) *Chem. Rev.* **1998**, *98*, 1−2 (Special Issue on Polyoxometalates; Hill, C. L., Ed.). (e) Müller, A.; Roy, S. *Coord. Chem. Rev.* **2003**, *245*, 153−166. (f) Cronin, L. In *Comprehensive Coordination Chemistry II*; McCleverty, J. A., Meyer, T. J., Eds.; Elsevier: Amsterdam, 2004; Vol.7, pp 1−56. (g) Hasenknopf, B.; Micoine, K.; Lacôte, E.; Thorimbert, S.; Malacria, M.; Thouvenot, R. *Eur. J. Inorg. Chem.* **2008**, 5001−5013. (h) Kortz, U.; Müller, A.; van Slageren, J.; Schnack, J.; Dalal, N. S.; Dressel, M. *Coord. Chem. Rev.* **2009**, *253*, 2315−2327. (i) *Eur. J. Inorg. Chem.* **2009**, *34* (Issue dedicated to Polyoxometalates; Kortz, U., Guest Ed.). (j) Long, D. L.; Tsunashima, R.; Cronin, L. *Angew. Chem., Int. Ed.* **2010**, *49*, 1736−1758. (k) Izarova, N. V.; Pope, M. T.; Kortz, U. *Angew. Chem., Int. Ed.* **2012**, *51*, 9492−9510. (l) Clemente-Juan, J. M.; Coronado, E.; Gaita-Ariño, A. *Chem. Soc. Rev.* **2012**, *41*, 7464−7478. (m) Lv, H.; Geletii, Y. V.; Zhao, C.; Vickers, J. W.; Zhu, G.; Luo, Z.; Song, J.; Lian, T.; Musaev, D. G.; Hill, C. L. *Chem. Soc. Rev.* **2012**, *41*, 7572−7589. (n) Pope, M. T.; Kortz, U. Polyoxometalates. In *Encyclopedia of Inorganic and Bioinorganic Chemistry*; Scott, R. A., Ed.; John Wiley: Chichester. DOI: 10.1002/9781119951438.eibc0185.pub2. Published 17th December 2012.

(2) (a) Galán-Mascarüs, J. R.; Gómez-García, C. J.; Borrás-Almenar, J. J.; Coronado, E. *Adv. Mater.* **1994**, *6*, 221−223. (b) Clemente-Juan, J.; Coronado, E.; Galán-Mascarós, J.; Gómez-García, C. *Inorg. Chem.*

**1999**, *38*, 55−63. (c) Anderson, T. M.; Neiwert, W. A.; Hardcastle, K. I.; Hill, C. L. *Inorg. Chem.* **2004**, *43*, 7353−7358. (d) Stowe, A. C.; Nellutla, S.; Dalal, N. S.; Kortz, U. *Eur. J. Inorg. Chem.* **2004**, 3792−3797. (e) Jabbour, D.; Keita, B.; Mbomekalle, I. M.; Nadjo, L.; Kortz, U. *Eur. J. Inorg. Chem.* **2004**, 2036−2044. (f) Kortz, U.; Nellutla, S.; Stowe, A. C.; Dalal, N. S.; Rauwald, U.; Danquah, W.; Ravot, D. *Inorg. Chem.* **2004**, *43*, 2308−2317. (g) Kortz, U.; Nellutla, S.; Stowe, A. C.; Dalal, N. S.; van Tol, J.; Bassil, B. S. *Inorg. Chem.* **2004**, *43*, 144−154. (h) Yamase, T.; Fukaya, K.; Nojiri, H.; Ohshima, Y. *Inorg. Chem.* **2006**, *45*, 7698−7704. (i) Zhang, Z. M.; Qi, Y. F.; Qin, C.; Li, Y. G.; Wang, E. B.; Wang, X. L.; Su, Z. M.; Xu, L. *Inorg. Chem.* **2007**, *46*, 8162−8169. (j) Zhao, J. W.; Zhang, J.; Zheng, S. T.; Yang, G. Y. *Chem. Commun.* **2008**, 570−572. (k) Fang, X.; Kögerler, P. *Chem. Commun.* **2008**, 3396−3398. (l) Fang, X.; Kögerler, P. *Angew. Chem., Int. Ed.* **2008**, *47*, 8123−8126.

(3) (a) Zimmermann, M.; Belai, N.; Butcher, R. J.; Pope, M. T.; Chubarova, E. V.; Dickman, M. H.; Kortz, U. *Inorg. Chem.* **2007**, *46*, 1737−1740. (b) Ritchie, C.; Streb, C.; Thiel, J.; Mitchell, S. G.; Miras, H. N.; Long, D.-L.; Boyd, T.; Peacock, R. D.; McGlone, T.; Cronin, L. *Angew. Chem., Int. Ed.* **2008**, *47*, 6881−6884. (c) Bassil, B. S.; Ibrahim, M.; Mal, S. S.; Suchopar, A.; Ngo Biboum, R.; Keita, B.; Nadjo, L.; Nellutla, S.; van Tol, J.; Dalal, N. S.; Kortz, U. *Inorg. Chem.* **2010**, *49*, 4949−4959. (d) Assran, A. S.; Izarova, N. V.; Kortz, U. *CrystEngComm* **2010**, *12*, 2684−2686. (e) Bassil, B. S.; Ibrahim, M.; Al-Oweini, R.; Asano, M.; Wang, Z.; van Tol, J.; Dalal, N. S.; Choi, K.-Y.; Biboum, R. N.; Keita, B.; Nadjo, L.; Kortz, U. *Angew. Chem., Int. Ed.* **2011**, *50*, 5961−5964. (f) Ismail, A. H.; Bassil, B. S.; Yassin, G. H.; Keita, B.; Kortz, U. *Chem.—Eur. J.* **2012**, *18*, 6163−6166.

(4) (a) Zheng, S.-T.; Yang, G.-Y. *Chem. Soc. Rev.* **2012**, *41*, 7623−7646. (b) Oms, O.; Dolbecq, A.; Mialane, P. *Chem. Soc. Rev.* **2012**, *41*, 7497−7536.

(5) Winter, R. S.; Yan, J.; Busche, C.; Mathieson, J. S.; Prescimone, A.; Brechin, E. K.; Long, D.-L.; Cronin, L. *Chem.—Eur. J.* **2013**, *19*, 2976−2981.

(6) Huang, L.; Cheng, L.; Fang, W.-H.; Wang, S.-S.; Yang, G.-Y. *Eur. J. Inorg. Chem.* **2013**, 1693−1698.

(7) Zhang, Z.-M.; Yao, S.; Li, Y.-G; Wu, H.-H.; Wang, Y.-H.; Rouzières, M.; Clérac, R.; Su, Z.-M.; Wang, E.-B. *Chem. Commun.* **2013**, *49*, 2515−2517.

(8) El Moll, H.; Rousseau, G.; Dolbecq, A.; Oms, O.; Marrot, J.; Haouas, M.; Taulelle, F.; Rivière, E.; Wernsdorfer, W.; Lachkar, D.; Lacôte, E.; Keita, B.; Mialane, P. *Chem.—Eur. J.* **2013**, *19*, 6753−6765.

(9) Rousseau, G.; Rivière, E.; Dolbecq, A.; Marrot, J.; Oms, O.; Mialane, P. *Eur. J. Inorg. Chem.* **2013**, 1793−1798.

(10) Zhang, Y.; Han, X.-B.; Zhang, Z.-M.; Liu, Z.-J.; Wang, E.-B. *Chin. Chem. Lett.* **2013**, *24*, 581−584.

(11) Zheng, Y.; Wen, R.; Kong, X.; Long, L.; Huang, R.; Zheng, L. *Dalton Trans.* **2012**, *41*, 9871−9875.

(12) Ibrahim, M.; Xiang, Y.; Bassil, B. S.; Lan, Y.; Powell, A. K.; de Oliveira, P.; Keita, B.; Kortz, U. *Inorg. Chem.* **2013**, *52*, 8399−8408.

(13) (a) Baker, L. C. W.; McCutcheon, T. P. *J. Am. Chem. Soc.* **1956**, *78*, 4503. (b) Baker, L. C. W.; Baker, V. E. S.; Eriks, K.; Pope, M. T.; Shibata, M.; Rollins, O. W.; Fang, J. H.; Koh, L. L. *J. Am. Chem. Soc.* **1966**, *88*, 2329−2331. (c) Andres, H.; Aebersold, M.; Güdel, H. U.; Clemente-Juan, J. M.; Coronado, E.; Büttner, H.; Kearley, D.; Zolliker, M. *Chem. Phys. Lett.* **1998**, *289*, 224−230.

(14) (a) Weakley, T. J. R.; Evans, H. T.; Showell, J. S., Jr.; Tourné, G. F.; Tourné, C. M. *J. Chem. Soc., Chem. Commun.* **1973**, *8*, 139−148. (b) Finke, R. G.; Droege, M. W.; Domaille, P. *J. Inorg. Chem.* **1987**, *26*, 3886−3896. (c) Casañ-Pastor, N.; Bas-Serra, J.; Coronado, E.; Pourroy, G.; Baker, L. C. W. *J. Am. Chem. Soc.* **1992**, *114*, 10380−10383. (d) Gómez-García, C. J.; Coronado, E.; Borrás-Almenar, J. *J. Inorg. Chem.* **1992**, *31*, 1667−1673. (e) Clemente-Juan, J. M.; Andres, H.; Aebersold, M.; Borrás-Almenar, J. J.; Coronado, E.; Güdel, H. U.; Büttner, H.; Kearly, G. *Inorg. Chem.* **1997**, *36*, 2244−2245. (f) Clemente-León, M.; Coronado, E.; Galán-Mascarüs, J.-R.; Gómez-García, C.; Gómez-García, C. J.; Fernández-Otero, T. *J. Mater. Chem.* **1998**, *8*, 309−312. (g) Andres, H.; Clemente-Juan, J. M.; Aebersold, M.; Güdel, H. U.; Coronado, E.; Büttner, H.; Kearly, G.; Melero, J.; Burriel, R. *J. Am. Chem. Soc.* **1999**, *121*, 10028−10034. (h) Bi, L.-H.; Wang, E.-B.; Peng, J.; Huang, R.-D.; Xu, L.; Hu, C.-W. *Inorg. Chem.* **2000**, *39*, 671−679. (i) Bi, L.-H.; Huang, R.-D.; Peng, J.; Wang, E.-B.; Wang, Y.-H.; Hu, C.-W. *J. Chem. Soc., Dalton Trans.* **2001**, 121−129. (j) Andres, H.; Clemente-Juan, J. M.; Basler, R.; Aebersold, M.; Güdel, H.-U.; Borrás-Almenar, J. J.; Gaita-Ariño, A.; Coronado, E.; Büttner, H.; Janssen, S. *Inorg. Chem.* **2001**, *40*, 1943−1950. (k) Clemente-Juan, M.; Coronado, E.; Gaita-Ariño, A.; Giménez-Saiz, C.; Chaboussant, G.; Güdel, H.-U.; Burriel, R.; Mutka, H. *Chem.—Eur. J.* **2002**, *8*, 5701−5708. (l) Ruhlmann, L.; Canny, J.; Contant, R.; Thouvenot, R. *Inorg. Chem.* **2002**, *41*, 3811−3819. (m) Clemente-Juan, J. M.; Coronado, E.; Gaita-Ariño, A.; Giménez-Saiz, C.; Güdel, H.-U.; Sieber, R.; Birche, R.; Mutka, H. *Inorg. Chem.* **2005**, *44*, 3389−3395. (n) Tan, R.; Pang, X.; Wang, H.; Cui, S.; Jiang, Y.; Wang, C.; Wang, X.; Song, W. *Inorg. Chem. Commun.* **2012**, *25*, 70−73. (o) Ruhlmann, L.; Schaming, D.; Ahmed, I.; Courville, A.; Canny, J.; Thouvenot, R. *Inorg. Chem.* **2012**, *51*, 8202−8211. (p) Kikukawa, Y.; Suzuki, K.; Yamaguchi, K.; Mizuno, N. *Inorg. Chem.* **2013**, *52*, 8644−8652.

(15) Tourné, C. M.; Tourné, G. F.; Zonnevijlle, F. *J. Chem. Soc., Dalton Trans.* **1991**, 143−155.

(16) Ritorto, M. D.; Anderson, T. M.; Neiwert, W. A.; Hill, C. L. *Inorg. Chem.* **2004**, *43*, 44−49.

(17) Lv, H.; Song, J.; Geletii, Y. V.; Guo, W.; Bacsa, J.; Hill, C. L. *Eur. J. Inorg. Chem.* **2013**, 1720−1725.

(18) Guo, J.; Zhang, D.; Chen, L.; Song, Y.; Zhu, D.; Xu, Y. *Dalton Trans.* **2013**, *42*, 8454−8459.

(19) Clemente-Juan, J. M.; Coronado, E.; Forment-Aliaga, A.; Galán-Mascarüs, J.-R.; Giménez-Saiz, C.; Gómez-García, C. *J. Inorg. Chem.* **2004**, *43*, 2689−2694.

(20) Lisnard, L.; Mialane, P.; Dolbecq, A.; Marrot, J.; Clemente-Juan, J. M.; Coronado, E.; Keita, B.; de Oliveira, P.; Nadjo, L.; Sécheresse, F. *Chem.—Eur. J.* **2007**, *13*, 3525−3536.

(21) Weakley, T. J. R. *J. Chem. Soc. Chem. Commun.* **1984**, 1406−1407.

(22) Lydon, C.; Sabi, M. M.; Symes, M. D.; Long, D.-L.; Murrie, M.; Yoshii, S.; Nojiri, H.; Cronin, L. *Chem. Commun.* **2012**, *48*, 9819−9821.

(23) (a) Mal, S. S.; Dickman, M. H.; Kortz, U.; Todea, A. M.; Merca, A.; Bögge, H.; Glaser, T.; Müller, A.; Nellutla, S.; Kaur, N.; van Tol, J.; Dalal, N. S.; Keita, B.; Nadjo, L. *Chem.—Eur. J.* **2008**, *14*, 1186−1195. (b) Bi, L.; Kortz, U.; Nellutia, S.; Stowe, A. C.; van Tol, J.; Dalal, N. S.; Keita, B.; Nadjo, L. *Inorg. Chem.* **2005**, *44*, 896−903. (c) Pichon, C.; Mialane, P.; Dolbecq, A.; Marrot, J.; Rivière, E.; Bassil, B. S.; Kortz, U.; Keita, B.; Nadjo, L.; Sécheresse, F. *Inorg. Chem.* **2008**, *47*, 11120−11128. (d) Mal, S. S.; Kortz, U. *Angew. Chem., Int. Ed.* **2005**, *44*, 3777−3780. (e) Mal, S. S.; Bassil, B. S.; Ibrahim, M.; Nellutla, S.; van Tol, J.; Dalal, N. S.; Fernández, J. A.; López, X.; Poblet, M. J.; Ngo Biboum, R.; Keita, B.; Kortz, U. *Inorg. Chem.* **2009**, *48*, 11636−11645. (f) Ibrahim, M.; Lan, Y.; Bassil, B. S.; Xiang, Y.; Suchopar, A.; Powell, A. K.; Kortz, U. *Angew. Chem., Int. Ed.* **2011**, *50*, 4708−4711. (g) Bassil, B. S.; Nellutla, S.; Kortz, U.; Stowe, A. C.; van Tol, J.; Dalal, N. S.; Keita, B.; Nadjo, L. *Inorg. Chem.* **2005**, *44*, 2659−2665.

(24) (a) Kortz, U.; Al-Kassem, N. K.; Savelieff, M. G.; Al Kadi, N. A.; Sadakane, M. *Inorg. Chem.* **2001**, *40*, 4742−4749. (b) Bassil, B. S.; Kortz, U.; Tigan, A. S.; Clemente-Juan, J. M.; Keita, B.; De Oliveira, P.; Nadjo, L. *Inorg. Chem.* **2005**, *44*, 9360−9368. (c) Bassil, B. S.; Dickman, M. H.; Reicke, M.; Kortz, U.; Keita, B.; Nadjo, L. *Dalton Trans.* **2006**, 4253−4259. (d) Nsouli, N. H.; Ismail, A. H.; Helgadottir, I. S.; Dickman, M. H.; Clemente-Juan, J. M.; Kortz, U. *Inorg. Chem.* **2009**, *48*, 5884−5890.

(25) (a) Aromí, G.; Brechin, E. K. *Struct. Bonding (Berlin)* **2006**, *122*, 1−67. and references therein. (b) Lehmann, J.; Gaita-Ariño, A.; Coronado, E.; Loss, D. *Nat. Nanotechnol.* **2007**, *2*, 312−317.

(26) Bogani, L.; Wernsdorfer, W. *Nat. Mater.* **2008**, *7*, 179−186.

(27) Timco, G. A.; Carretta, S.; Troiani, F.; Tuna, F.; Pritchard, R. J.; Muryn, C. A.; McInnes, E. J. L.; Ghirri, A.; Candini, A.; Santini, P.; Amoretti, G.; Affronte, M.; Winpenny, R. E. P. *Nat. Nanotechnol.* **2009**, *4*, 173−178.

(26) (a) Lis, T. *Acta Crystallogr.* **1980**, *B36*, 2042−2046. (b) Sessoli, R.; Gatteschi, D.; Caneschi, A.; Novak, M. A. *Nature* **1993**, *365*, 141−143.
(27) Yang, E. C.; Hendrickson, D. N.; Wernsdorfer, W.; Nakano, M.; Zakharov, L. N.; Sommer, R. D.; Rheingold, A. L.; Ledezma-Gairaud, M.; Christou, G. *J. Appl. Phys.* **2002**, *91*, 7382−7384.
(28) (a) Murrie, M.; Teat, S. J.; Stoeckli-Evans, H.; Güdel, H. U. *Angew. Chem., Int. Ed.* **2003**, *42*, 4653−4656. (b) Zhang, Y.-Z.; Wernsdorfer, W.; Pan, F.; Wang, Z.-M.; Gao, S. *Chem. Commun.* **2006**, 3302−3304. (c) Galloway, K. W.; Whyte, A. M.; Wernsdorfer, W.; Sanchez-Benitez, J.; Kamenev, K. V.; Parkin, A.; Peacock, R. D.; Murrie, M. *Inorg. Chem.* **2008**, *47*, 7438−7442. (d) Moubaraki, B.; Murray, K. S.; Hudson, T. A.; Robson, R. *Eur. J. Inorg. Chem.* **2008**, 4525−4529. (e) Klöwer, F.; Lan, Y.; Nehrkorn, J.; Waldmann, O.; Anson, C. E.; Powell, A. K. *Chem.—Eur. J.* **2009**, *15*, 7413−7422. (f) Murrie, M. *Chem. Soc. Rev.* **2010**, *39*, 1986 and references therein. (g) Scheurer, A.; Ako, A. M.; Saalfrank, R. W.; Heinemann, F. W.; Hampel, F.; Petukhov, K.; Gieb, K.; Stocker, M.; Müller, P. *Chem. Eur. J.* **2010**, *16*, 4784−4792.
(29) El Moll, H.; Dolbecq, A.; Marrot, J.; Rousseau, G.; Haouas, M.; Taulelle, F.; Guillaume, R.; Wernsdorfer, W.; Keita, B.; Mialane, P. *Chem.—Eur. J.* **2012**, *18*, 3845−3849.
(30) (a) Forment-Aliaga, A.; Coronado, E.; Feliz, M.; Gaita-Ariño, A.; Llusar, R.; Romero, F. M. *Inorg. Chem.* **2003**, *42*, 8019−8027. (b) AlDamen, M. A.; Clemente-Juan, J. M.; Coronado, E.; Martí-Gastaldo, C.; Gaita-Ariño, A. *J. Am. Chem. Soc.* **2008**, *130*, 8874−8875. (c) Ritchie, C.; Ferguson, A.; Nojiri, H.; Miras, H. N.; Song, Y.-F.; Long, D.-L.; Burkholder, E.; Murrie, M.; Kögerler, P.; Brechin, E. K.; Cronin, L. *Angew. Chem., Int. Ed.* **2008**, *47*, 5609−5612. (d) AlDamen, M. A.; Cardona-Serra, S.; Clemente-Juan, J. M.; Coronado, E.; Gaita-Ariño, A.; Martí-Gastaldo, C.; Luis, F.; Montero, O. *Inorg. Chem.* **2009**, *48*, 3467−3479. (e) Wu, Q.; Li, Y. G.; Wang, Y. H.; Clérac, R.; Lu, Y.; Wang, E. B. *Chem. Commun.* **2009**, 5743−5745. (f) Wu, Q.; Li, Y.; Wang, Y.; Wang, E.; Zhang, Z.; Clérac, R. *Inorg. Chem.* **2009**, *48*, 1606−1612. (g) Compain, J.-D.; Mialane, P.; Dolbecq, A.; Mbomekalle, I. M.; Marrot, J.; Sécheresse, F.; Rivière, E.; Rogez, G.; Wernsdorfer, W. *Angew. Chem., Int. Ed.* **2009**, *48*, 3077−3081. (h) Fang, X.; Speldrich, M.; Schilder, H.; Cao, R.; O'Halloran, K. P.; Hill, C. L.; Kogerler, P. *Chem. Commun.* **2010**, *46*, 2760−2762. (i) Feng, X.; Zhou, W.; Li, Y.; Ke, H.; Tang, J.; Clérac, R.; Wang, Y.; Su, Z.; Wang, E. *Inorg. Chem.* **2012**, *51*, 2722−2724.
(31) (a) du Peloux, C.; Dolbecq, A.; Mialane, P.; Marrot, J.; Riviere, E.; Secheresse, F. *Angew. Chem., Int. Ed.* **2001**, *40*, 2455−2457. (b) Ma, Y.; Li, Y. G.; Wang, E. B.; Lu, Y.; Xu, X.; Bai, X. L. *Transition Met. Chem.* **2006**, *31*, 262−267.
(32) (a) Mbomekallé, I.-M.; López, X.; Poblet, J. M.; Sécheresse, F.; Keita, B.; Nadjo, L. *Inorg. Chem.* **2010**, *49*, 7001−7006. (b) Wang, Y.; Zheng, G.; Morokuma, K.; Geletii, Y. V.; Hill, C. L.; Musaev, D. G. *Phys. Chem. B* **2006**, *110*, 5230−5237. (c) Pope, M. T.; Papaconstantinou, E. *Inorg. Chem.* **1967**, *6*, 1147−1152. (d) Papaconstantinou, E.; Pope, M. T. *Inorg. Chem.* **1967**, *6*, 1152−1155. (e) Pope, M. T.; Varga, G. M., Jr. *Inorg. Chem.* **1966**, *5*, 1249−1254.
(33) Hervé, G.; Tézé, A. *Inorg. Chem.* **1977**, *16*, 2115−2117.
(34) *SAINT*; Bruker AXS Inc.: Madison, WI, 2007.
(35) (a) Sheldrick, G. M. *Acta Crystallogr., Sect A* **2007**, *64*, 112−122. (b) Sheldrick, G. M. *SADABS*; University of Göttingen: Göttingen, Germany, 1996.
(36) Sheldrick, G. M. *SHELX-97/2013, Program for Solution of Crystal Structures*; University of Göttingen: Göttingen, Germany, 1997, 2013.
(37) Keita, B.; Nadjo, L. *J. Electroanal. Chem.* **1988**, *243*, 87−103.
(38) Brown, I. D.; Altermatt, D. *Acta Crystallogr., Sect. B* **1985**, *41*, 244−247.
(39) (a) Müller, A.; Döring, J. *Z. Anorg. Allg. Chem.* **1991**, *595*, 251−274. (b) Zhao, J.; Zhang, J.; Zheng, S.; Yang, G. *Inorg. Chem.* **2007**, *46*, 10944−10946. (c) Al-Kadamany, G.; Hussain, F.; Mal, S. S.; Dickman, M. H.; Leclerc-Laronze, N.; Marrot, J.; Cadot, E.; Kortz, U. *Inorg. Chem.* **2008**, *47*, 8574−8576.
(40) Kostakis, G. E.; Powell, A. K. *Coord. Chem. Rev.* **2009**, *253*, 2686−2697.
(41) Kostakis, G. E.; Blatov, V. A.; Proseprio, D. M. *Dalton Trans.* **2012**, *41*, 4634−4640.
(42) Alexandrov, E. V.; Blatov, V. A.; Kochetkov, A. V.; Proserpio, D. M. *CrystEngComm* **2011**, *13*, 3947−3958.
(43) Kostakis, G. E.; Powell, A. K. *Chem.—Eur. J.* **2010**, *16*, 7983−7989.
(44) Ilyushin, G. D.; Blatov, V. A. *Acta Crystallogr., Sect. B* **2009**, *65*, 300−307.
(45) Kostakis, G. E.; Ako, A. M.; Powell, A. K. *Chem. Soc. Rev.* **2010**, *39*, 2238−2271.
(46) Kostakis, G. E.; Blatov, V. A.; Proserpio, D. M.; Perlepes, S. P.; Powell, A. K. *Coord. Chem. Rev.* **2009**, *256*, 1246−1278.
(47) Wix, P.; Kostakis, G. E.; Blatov, V. A.; Proserpio, D. M.; Perlepes, S. P.; Powell, A. K.; Eur, J. *Inorg. Chem.* **2013**, 520−526.
(48) Keita, B.; Nadjo, L. Electrocatalysis of Inorganic Chemicals by Chemically Modified Electrodes. In *Encyclopedia of Electrochemistry*; Bard, A. J., Stratmann, M., Eds.; Wiley-VCH: 2007; Vol. *10*, pp 705−728.
(49) (a) Toth, J. E.; Anson, F. C. *J. Electroanal. Chem.* **1988**, *256*, 361−370. (b) Bi, L.-H.; Kortz, U.; Keita, B.; Nadjo, L. *J. Chem. Soc., Dalton Trans.* **2004**, 3184−3190. (c) Bi, L.-H.; Kortz, U.; Dickman, M. H.; Keita, B.; Nadjo, L. *Inorg. Chem.* **2005**, *44*, 7485−7493.
(50) Sadakane, M.; Steckhan, E. *J. Mol. Catal. Chem.* **1996**, *114*, 221.
(51) Keita, B.; Mialane, P.; Sécheresse, F.; de Oliveira, P.; Nadjo, L. *Electrochem. Commun.* **2007**, *9*, 164.
(52) (a) Stracke, J. J.; Finke, R. G. *J. Am. Chem. Soc.* **2011**, *133*, 1472 and references therein. (b) Stracke, J. J.; Finke, R. G. *ACS Catal.* **2013**, *3*, 1209.